



HAL
open science

Thermomechanical Coupling & Dynamic Crack Propagation

Z Soumahoro, H. Maigre

► **To cite this version:**

Z Soumahoro, H. Maigre. Thermomechanical Coupling & Dynamic Crack Propagation. Universal Journal of Fracture Mechanics, 2016, 4, pp.70 - 85. hal-01614798

HAL Id: hal-01614798

<https://hal.science/hal-01614798v1>

Submitted on 11 Oct 2017

HAL is a multi-disciplinary open access archive for the deposit and dissemination of scientific research documents, whether they are published or not. The documents may come from teaching and research institutions in France or abroad, or from public or private research centers.

L'archive ouverte pluridisciplinaire **HAL**, est destinée au dépôt et à la diffusion de documents scientifiques de niveau recherche, publiés ou non, émanant des établissements d'enseignement et de recherche français ou étrangers, des laboratoires publics ou privés.

Thermomechanical Coupling & Dynamic Crack Propagation

Z. Soumahoro^{1,2}, H. Maigre¹

¹École Polytechnique

Département de Mécanique, LMS - UMR CNRS 7649

91 128 Palaiseau Cedex, France

(zoumana.soumahoro, hubert.maigre)@polytechnique.edu

²Institut National Polytechnique Félix Houphouët-Boigny (INPHB),

Département Génie Mécanique et Energétique

BP 1093 Yamoussoukro, Côte d'Ivoire

zoumana.soumahoro@inphb.edu.ci

Abstract

Thermomechanical coupling is studied in dynamic fracture mechanisms. The crack propagation problem is formalized within the framework of the thermodynamics of irreversible processes to determine their essential parameters and couplings. The analytical approach developed herein is based on the linear elastic mechanics of fracture, including the inertial effects and thermomechanical couplings. For a one-dimensional restriction, the mechanics and thermics equations are uncoupled in the entire structure, with simplified thermomechanical coupling at the crack-tip. This study aims to determine the criteria for fracture initiation and propagation in the presence of heating and inertial effects.

Key Word and Phrases

Thermomechanical Coupling, Dynamic Fracture, Crack Propagation, Propagation Criteria, Temperature at Crack-tip.

1. Introduction

Thermomechanical coupling in dynamic crack propagation has attracted considerable experimental and theoretical interest in recent years. Döll [6] and Shockey et al. [7] used thermocouples for temperature measurements. Fuller et al. [8] measured the temperature increase at a mobile fast ($200 - 650 \text{ m.s}^{-1}$) crack-tip in poly(methyl methacrylate) using an infrared detector. They also used thermocouples and thermosensitive liquid crystal films to measure the heat generated relative to the crack speed. Bui et al. [3] used an infrared camera to film the temperature field in a fissured thin plate at low propagation velocity (2 mm.s^{-1}). They detected a temperature rise of approximately 10°C at the crack-tip. Furthermore, Weichert and Schönert [9], [10], Rice and Levy [11], and several others attempted to theoretically estimate the temperature at the crack-tip. Because the origin of heat at the crack-tip is dependent on plastic dissipation, the most accurate models of temperature fields are based on the capacity to calculate the mechanics fields related to crack propagation. However, exact analytical solutions for plastic field work in the crack propagation zone are not available even for perfect elastoplastic materials. Moreover, despite intense research efforts toward understanding the dynamic fracture process, few studies have systematically combined experimental and theoretical models to validate the experimental measurement techniques or theory that serves as the basis for such investigations. The successful modelling of complex loading environments and the constitutive laws of these experiments remain an open problem. Thus, in the present study, a detailed theoretical analysis was conducted to understand the nature of this coupling. An entirely coupled assay (temperature-displacement or temperature-time) was conducted to model these experiments. To clarify the evolution of the temperature field, one-dimensional modelling was performed to facilitate the understanding and study of its influence on propagation conditions. This is primarily applicable to metals and polymers. While this phenomenon finds increasing applications, its properties remain poorly known, especially under dynamic loading.

2. Thermodynamic Description of Crack Propagation

Fracture is a process in which much energy is wasted. A solid in which a crack propagates represents a system in this process, and dissipation is mainly due to various mechanisms such as internal friction and plastic deformation. The evolution of such a system can be described according to the thermodynamics laws for continuous media. For any material system, the first and second principles of thermodynamics can be expressed as follows:

$$\begin{cases} \dot{E} + \dot{C} = P_{ex} + P_{cr} & (\text{Energy balance}) \\ \dot{S} + \int_{\partial V} \frac{q \cdot n}{T} da \geq 0 & (\text{Entropy production}) \end{cases} \quad (2.1)$$

where $E, C, P_{ex}, P_{Cr}, S,$ and q denote the internal energy, kinetic energy, power of external forces, received calorific power, entropy, and heat flux, respectively.

In the interest of simplicity, the problem of linear crack propagation is considered in two dimensions (plane strain, plane stress, or shearing anti-plane); however, the material is unspecified. A thermally isolated system is also considered. As shown in Fig.1, the applied force $F(t)$ and displacement $u(t)$ are on complementary parts $\partial\Omega_u$ and $\partial\Omega_F$ of the border. On the crack surface Σ , the free edge condition is also considered. Because of the presence of the possible mobile singularity of the thermomechanical fields close to the crack-tip A , the thermomechanical description is not traditional. The additional terms due to the singularity can play a fundamental role.

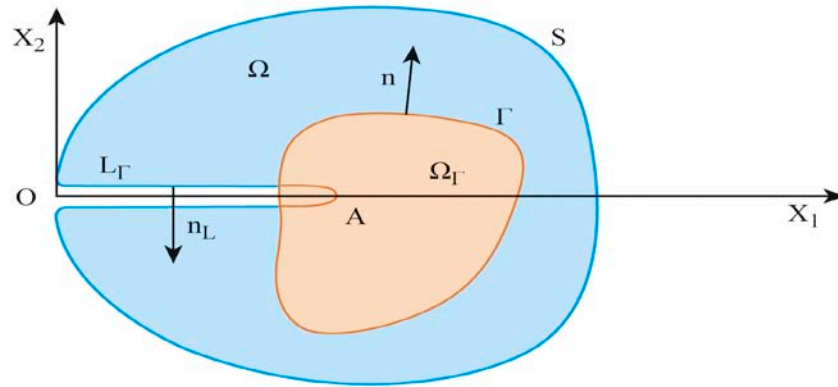


Fig. 1 Linear crack with mobile reference.

The consequence of the energy balance can be established as follows: If $\xi, T,$ and S denote the specific internal energy, temperature, and specific entropy, respectively, the energy balance of the entire system can be written as:

$$\frac{d}{dt} \int_{\Omega} \rho \left(\xi + \frac{1}{2} \dot{u}^2 \right) d\Omega = \int_{\partial\Omega} n \cdot \sigma \cdot \dot{u} da + P_{cr} \quad (2.2)$$

Although the expression on the right-hand side of (2.2) is clear, that on the left-hand side is not commonplace as the function $\rho \left(\xi + \frac{1}{2} \dot{u}^2 \right)$ is not necessarily integrable because of the mobile singularity. It is necessary to isolate the crack-tip with a closed curve Γ in the translatory movement of the crack that delimits the domain V_{Γ} .

In the mobile reference AX_1X_2 , we introduce the temporal derivative $(\dot{\cdot})$, $\dot{\xi} = \xi_{,t}(X_1, X_2, t)$, which is related to the material derivative $(\dot{\cdot})$ by the relation : [12]

$$\dot{\xi}' - \dot{a} \cdot \xi_{,1} = \dot{\xi} \quad (2.3)$$

The principle of singularity transport consists of the conservation of the singularity nature with

the movement of the crack. While $\dot{\xi}$ can be singular, $\dot{\xi}'$ is much more regular, and $\dot{\xi}': -\dot{a} \xi_1$. Because of this regularity, we obtain:

$$\frac{d}{dt} \int_{V_\Gamma} \rho \left(\xi + \frac{1}{2} \dot{u}^2 \right) d\Omega = \int_{V_\Gamma} \rho (\dot{\xi} + \dot{u} \ddot{u}) d\Omega$$

and thus, for an evanescent curve, $\Gamma \rightarrow 0$

$$\lim_{\Gamma \rightarrow 0} \frac{d}{dt} \int_{V_\Gamma} \rho \left(\xi + \frac{1}{2} \dot{u}^2 \right) d\Omega = 0 \quad (2.4)$$

From

$$\frac{d}{dt} \int_{V_\Gamma} \rho \left(\xi + \frac{1}{2} \dot{u}^2 \right) d\Omega = \int_{\Omega_\Gamma} \rho (\dot{\xi} + \dot{u} \ddot{u}) d\Omega - \int_\Gamma \rho \left(\xi + \frac{1}{2} \dot{u}^2 \right) \dot{a} n_1 d\Gamma$$

we finally obtain the energy balance of the entire system:

$$\lim_{\Gamma \rightarrow 0} \left(\int_{\Omega_\Gamma} n \cdot \sigma \cdot \dot{u} d\Omega - \int_{\Omega_\Gamma} \rho (\dot{\xi} + \dot{u} \ddot{u}) d\Omega + \int_\Gamma \rho \left(\xi + \frac{1}{2} \dot{u}^2 \right) \dot{a} n_1 d\Gamma \right) = 0 \quad (2.5)$$

To specify the energy exchanges close to the crack-tip, we compare (2.5) with the energy balance of the system occupying material items Ω_Γ at time t . This energy balance is given as

$$\int_{\Omega_\Gamma} \rho (\dot{\xi} + \dot{u} \ddot{u}) d\Omega = \int_{\partial\Omega} n \cdot \sigma \cdot \dot{u} da - \int_\Gamma n \cdot \sigma \cdot \dot{u} d\Gamma + \int_\Gamma q \cdot n d\Gamma \quad (2.6)$$

and then:

$$\lim_{\Gamma \rightarrow 0} \left(\int_\Gamma q \cdot n d\Gamma - \int_\Gamma \left[\rho \left(\xi + \frac{1}{2} \dot{u}^2 \right) \dot{a} n_1 + n \cdot \sigma \cdot \dot{u} \right] d\Gamma \right) = 0 \quad (2.7)$$

A quantity not necessarily null Π and defined as:

$$\Pi = \lim_{\Gamma \rightarrow 0} \int_\Gamma q \cdot n d\Gamma \quad (2.8)$$

physically represents a heat source concentrated at the crack-tip.

From (2.7), the expression for Π is given by:

$$\Pi = \lim_{\Gamma \rightarrow 0} \int_\Gamma \left[\rho \left(\xi + \frac{1}{2} \dot{u}^2 \right) \dot{a} n_1 + n \cdot \sigma \cdot \dot{u} \right] d\Gamma \quad (2.9)$$

The consequence of the second principle can also be deduced similarly. The entropy production of the entire system is reduced to $\dot{S} = \frac{d}{dt} \int_{\Omega} \rho s d\Omega$ and can then be expressed as:

$$S = \lim_{\Gamma \rightarrow 0} \left(\int_{\Omega_\Gamma} \rho \dot{s} d\Omega - \int_\Gamma \rho s \dot{a} n_1 d\Gamma \right) \geq 0 \quad (2.10)$$

To identify the entropy production at the crack-tip S_A , we can compare it to the entropy production of the material points system occupying Ω_Γ at time t :

$$S_\Gamma = \int_{\Omega_\Gamma} \rho \dot{s} d\Omega - \int_\Gamma \frac{q \cdot n}{T} d\Gamma \geq 0$$

which finally involves

$$S_A = \lim_{\Gamma \rightarrow 0} \int_{\Omega_\Gamma} \frac{1}{T} (q \cdot n - \rho T s \dot{a} n_1) d\Gamma \geq 0 \quad (2.11)$$

If $T \rightarrow T_A < +\infty$ when $X \rightarrow A$, it follows from (2.8), (2.9), and (2.11) that:

$$T_A \cdot S_A = \lim_{\Gamma \rightarrow 0} \int_\Gamma \left[\rho \left(\Psi + \frac{1}{2} \dot{u}^2 \right) \dot{a} n_1 + n \cdot \sigma \cdot \dot{u} \right] d\Gamma \geq 0 \quad (2.12)$$

where $\Psi = \xi - T s$ denotes the specific density of free energy and $D = T_A \cdot S_A$, the dissipation at

the crack-tip.

If $\dot{a} > 0$, from $\dot{\xi} : -\dot{a} \xi_{,1}$, we note that:

$$\begin{cases} \Pi = \dot{a} \Pi_A & \text{avec } \Pi_A = \lim_{\Gamma \rightarrow 0} \int_{\Gamma} \left[\rho \left(\xi + \frac{1}{2} \dot{u}^2 \right) n_1 - n \cdot \sigma \cdot u_{,1} \right] d\Gamma \\ D = \dot{a} G_A & G_A = \lim_{\Gamma \rightarrow 0} \int_{\Gamma} \left[\rho \left(\Psi + \frac{1}{2} \dot{u}^2 \right) n_1 - n \cdot \sigma \cdot u_{,1} \right] d\Gamma \end{cases} \quad (2.13)$$

In most applications, $T_A < +\infty$ and $s = r^{-1}$ (in terms of singularity); the fact that $\lim_{\Gamma \rightarrow 0} \int_{\Gamma} \rho T s n_1 d\Gamma = 0$ implies:

$$\Pi = D = \dot{a} G_A \geq 0 \quad (2.14)$$

Thus, the heat source also dissipates at the crack-tip. The fracture energy G is identified by the thermodynamic force Π_A in isentropic transformation and by the thermodynamic force G_A in isothermal transformation.

In fact, in the preceding analysis, continuity and regularity are tacitly allowed in all structures except at the crack-tip. If shock waves are present in the form of a discontinuity surface S being propagated in translation with the crack, the traditional equations of the surface discontinuity jump lead to the introduction of the heat surface and entropy production surface on S . In particular, the contribution of a discontinuity surface in translation with the crack is:

$$S_S = \dot{a} \lim_{\Gamma \rightarrow S} \int_{\Gamma} \frac{1}{T} \left[\rho \left(\Psi + \frac{1}{2} \dot{u}^2 \right) n_1 - n \cdot \sigma \cdot u_{,1} \right] d\Gamma \quad (2.15)$$

in terms of entropy production.

In conclusion, the singularity at the crack-tip leads to the introduction of a concentrated heat source Π in addition to the more traditional concepts of voluminal heat source $\sigma \dot{\varepsilon} - \rho \dot{\xi}$ and of surface heat sources localized on the discontinuity surface.

The thermomechanical evolution of solids is then described by mechanical equations (equilibrium, constitutive laws) and thermal equations that simply express the various conditions of the sources. These thermal equations are:

$$\left\{ \begin{array}{l} \bullet \text{Local equations} \quad : \quad \forall x \in \Omega \quad \text{div } q = \sigma \dot{\varepsilon} - \rho \dot{\xi} \\ \bullet \text{Boundary conditions} \quad : \quad \cdot \text{Classical on } \partial\Omega \\ \quad \quad \quad \quad \quad \quad \quad \cdot \text{Non-classical at the crack-tip } A \\ \lim_{\Gamma \rightarrow 0} \int_{\Gamma} q \cdot n \, d\Gamma = \Pi \end{array} \right. \quad (2.16)$$

3. Thermal Analysis

Thermomechanical coupling occurs at different levels: local coupling at a regular point by the energy balance $\text{Div } q = \sigma \dot{\varepsilon} - \rho \dot{\xi}$ as well as coupling at the crack-tip by (2.8) and (2.9), notwithstanding the fact that the constitutive laws also imply the temperature.

The most interesting question is naturally the asymptotic behaviour of the thermomechanical response. It is clear that for most materials, the coupled equations are so complex that analytical solutions cannot be explicitly obtained. However, partial results can be established when it is assumed that conduction obeys the Fourier law:

$$q = -k \cdot \nabla T \quad (3.1)$$

In this case, we establish what follows [3]. If the material is elastic, the free energy density

$\Psi(\varepsilon, T)$ can be expressed as:

$$\rho\Psi = \frac{1}{2}(\lambda\varepsilon_{ii}\varepsilon_{kk} + 2\mu\varepsilon_{ij}\varepsilon_{ij}) - 3K\alpha(T - T_0) - cT\text{Log}\left(\frac{T}{T_0}\right) - (S_0 - c)T + \Psi_0 \quad (3.2)$$

and the constitutive laws are:

$$\begin{cases} S = -\frac{\partial\Psi}{\partial T} \Rightarrow \rho S = 3K\alpha\varepsilon_{kk} + c\text{Log}\left(\frac{T}{T_0}\right) + S_0 \\ \sigma = \rho\frac{\partial\Psi}{\partial\varepsilon} \Rightarrow \sigma_{ij} = \lambda\varepsilon_{ii}\delta_{ij} + 2\mu\varepsilon_{ij} - 3K\alpha(T - T_0)\delta_{ij} \end{cases} \quad (3.3)$$

where $K = \frac{1}{3}(3\lambda + 2\mu)$ is the bulk modulus, and λ and μ are Lamé's coefficients.

The thermomechanical equations of dynamic crack propagation can now be explicitly written as:

$$\begin{cases} k\Delta T - c\rho\dot{T} - 3K\alpha T_0 \text{tr}\dot{\varepsilon} + \dot{a}G\delta = 0 \\ (\lambda + \mu)\nabla\text{tr}\varepsilon + \mu\Delta u - 3K\alpha\nabla T - \rho\ddot{u} + F = 0 \end{cases} \quad (3.4)$$

where $T, \varepsilon, \alpha, c, k,$ and δ denote the temperature field, deformation field, bulk heat, linear dilatation coefficient, and Dirac mass at crack-tip, respectively.

Thus, we observe, on the one hand, a double interaction between the thermal and the mechanical effects with traditional thermoelastic coupling at any point in the solid, and, on the other hand, a new thermomechanical coupling arising from the creation of a heat source by mechanical energy dissipation at the extremity of a propagating crack.

The study of the asymptotic behaviour of the thermomechanical response is formulated as follows. The displacement u and temperature T are developed like a series of decreasing singularities:

$$\begin{cases} u = u^{(1)} + \kappa u^{(2)} + \dots \\ T = T^{(1)} + \kappa T^{(2)} + \dots \end{cases} \quad (3.5)$$

where κ is a small positive parameter, and $u^{(n)}$ and $T^{(n)}$ belong to the entirety of elementary functions:

$$r^\beta (\text{Log } r)^{\beta_1} \dots (\text{Log}_m r)^{\beta_m} f(\theta, t)$$

where β_1 and β_2 are real numbers and $(\text{Log}_m r) = \text{Log}(\text{Log}_{m-1} r)$, $f(\theta, t)$, which represents the angular distribution, is supposed to be regular on the interval $]-\pi, \pi[$ with regard to θ .

The time derivative in (3.4) can be asymptotically evaluated because for any physical quantity Z we obtain:

$$\dot{Z} = -\dot{a}Z_{,1} + \text{more regular term} \quad (3.6)$$

The development (3.5) is now deduced point-by-point from equations (3.1) and (3.4) and appropriate boundary conditions on the crack-tip.

First, it is supposed that $\Pi \neq 0$, and thus, from the previous discussion, we obtain:

$$T^{(1)} = -\frac{\dot{a}G}{2k\pi} \text{Log } r + T_0 + O(\sqrt{r} \text{Log } r) \quad (3.7)$$

where T_0 is a uniform temperature distribution. The singularity of the temperature field of the first order is thus logarithmic.

However, the claim $\Pi \neq 0$ also implies from (2.8), (2.9), and (3.2) that $\varepsilon^{(1)}$ is more singular than $T^{(1)}$. Under these conditions, $u^{(1)}$ necessarily verifies the local equation:

$$(\lambda + \mu) \nabla \text{tr} \varepsilon^{(1)} + \mu \Delta u^{(1)} - \rho \dot{a}^2 u_{,11}^{(1)} = 0 \quad (3.8)$$

as it follows from (3.5). (3.8) is not new because it exactly represents the classical form studied in isothermal elastodynamics by Yoffé [4], [19], [20]. By the analytical method, it is well known that the solution $u^{(1)}$ is a linear combination of the elementary functions $K_i(t) Z(\dot{a}) r^{\frac{1}{2}} h_{ij}(\theta, \dot{a})$, which effectively leads to $\Pi \neq 0$.

From the expressions obtained for $T^{(1)}$ and $u^{(1)}$, (3.4) proves that $T^{(2)}$ must satisfy:

$$k \Delta T^{(2)} + 3 K \alpha T^{(1)} \dot{a} (\text{tr} \varepsilon^{(1)})_{,1} = 0, \quad (3.9)$$

and we obtain:

$$T^{(2)} = \bar{T}(t) + r^{\frac{1}{2}} \text{Log } r f(\theta, \dot{a}) \quad (3.10)$$

with mode I of loading and the boundary conditions being perfectly isolated:

$$f(\theta, \dot{a}) = - \frac{3 K \alpha \left(2 - \frac{\rho}{\lambda + 2 \mu} \dot{a}^2 \right) \left(\zeta - \sqrt{1 - \frac{\rho}{\lambda + 2 \mu} \dot{a}^2} \right)}{\pi^{\frac{3}{2}} \sqrt{2} \rho k^2 (\lambda + 2 \mu)} K_i \dot{a}^2 G \cos \frac{\theta}{2} \quad (3.11)$$

where ζ is proportional to $\frac{\beta_1}{\beta_2}$ as defined in [4, 5].

The process generating the temperature field can be highlighted by the layout of isotherms:

$$T^{(1)} + \kappa T^{(2)} = Cte$$

We use the physical characteristics of polyethylene and steel.

The data in Table 1 defines the characteristic length l :

$$l^2 = \frac{k (\lambda + \mu)}{3 K \alpha K_{ld} \frac{\mu}{\rho}}$$

Table 1 Physical characteristics of polyethylene and steel

		Polyethylene	Steel
λ	$[N.m^{-2}]$	$1,1.10^9$	$0,8.10^{11}$
μ	$[N.m^{-2}]$	$0,3.10^9$	$0,8.10^{11}$
k	$[W.m^{-1}.K^{-1}]$	0,35	42,0
α	$[K^{-1}]$	$200,0.10^{-6}$	$1,5.10^{-5}$
K_{ld}	$[N.m^{\frac{3}{2}}]$	$2,0.10^6$	$1,0.10^7$

This value corresponds to several interatomic distances, and therefore, it must necessarily be placed at much larger distances in front of l to ensure the validity of the thermodynamics equations

of continuous media. In addition, $\frac{r}{l}$ should not be too large so that the asymptotic developments make sense. We then take $\frac{r}{l} : 100 \text{ to } 1000$. To trace the isotherms, we set $G = \frac{1-\nu^2}{E} K_{Ia}^2$, which corresponds to an energetic criterion of propagation.

The principal part of the temperature $T^{(1)}$ is a revolution field determined by the rate G at which heat is dissipated by conduction. Reciprocally, the knowledge of the temperature field makes it possible to determine G ; however, it does not allow the heat dissipation regime to be deduced. Thus, from $T^{(2)}$, the angular distributions $f(\theta, \dot{a})$ can be easily seen in Fig.2, which is in agreement with the results of [13] for $\dot{a} = 100 \text{ m.s}^{-1}$ with regard to steel. These results show a temperature field dominated by adiabaticity for $r > 0.001 \text{ m}$, with the direction of the isotherms being parallel to the crack line ($\theta = 0$).

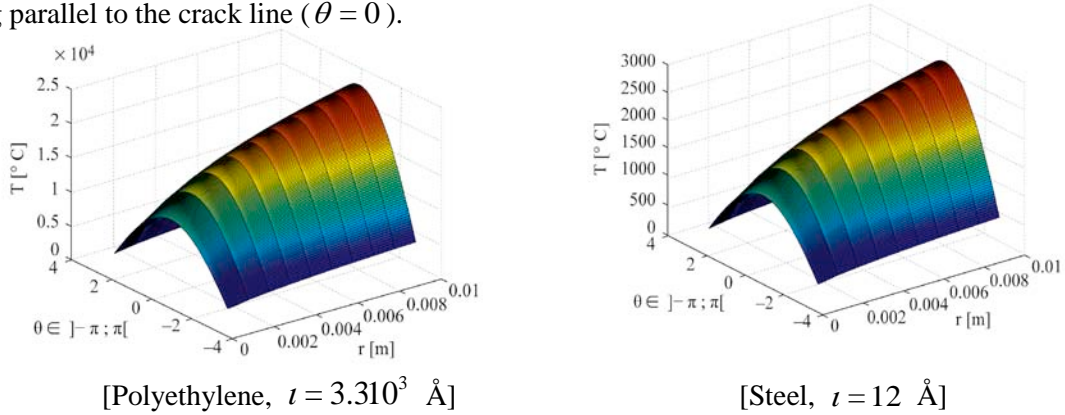


Fig.2 Temperature distribution $T^{(2)}$, $\dot{a} = 100 \text{ m.s}^{-1}$.

Fig.3 shows the isothermal curves $T^{(1)} + \kappa T^{(2)}$ with $r = 0.001 \text{ m}$ until a constant $\bar{T}(t)$, with different crack propagation velocity \dot{a} for polyethylene and steel. It shows that these isotherms depend slightly on the speed \dot{a} in the interval $]0, C_r[$.

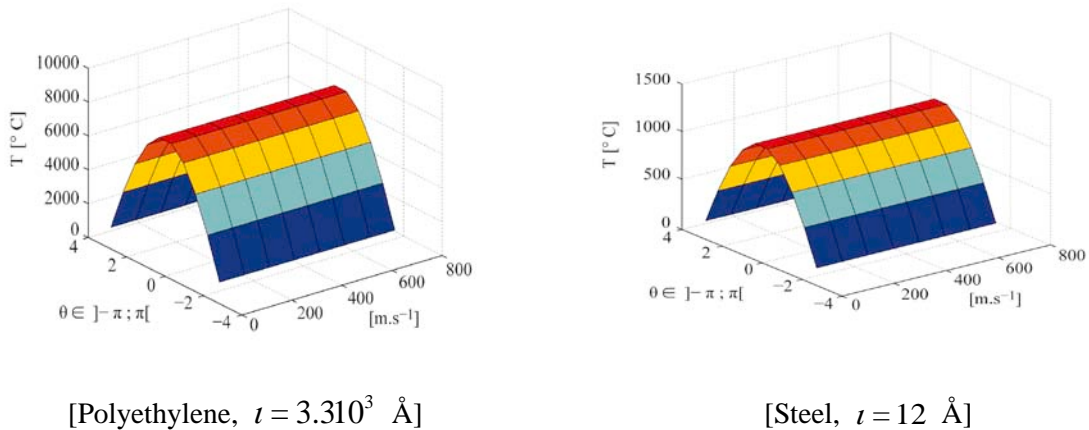


Fig.3 Isothermal curves as function of \dot{a} , $r = 0.001 \text{ m}$.

The direction of the isotherms, which is appreciably parallel to the crack line, shows that the process is essentially adiabatic, thus corroborating the results of [15].

The model adopts the assumption of brittle fracture, in which all rupture phenomena are concentrated at a mathematical singularity. In the calculation, therefore, any reference to plasticity can be avoided, and a very simple thermal analysis of the phenomenon is enabled. The thermal singularity must be considered a mathematical singularity exactly as we interpret a singularity in mechanical fields. It is clear that, physically, no material would support an infinite constraint or deformation and an infinite temperature. The model previsions appear to agree rather well with the experimental results except for a certain radius ι . Thus, it is necessary to use many simplifying assumptions to analytically study the initially posed problem.

4. One-dimensional Modelling

Based on the theoretical analysis, the objective is to, on the one hand, study the coupling effect, and, on the other hand, analyse the criteria in the function of the temperature and their effects on dynamic crack propagation [4]. This is not numerically possible in $2D$ because the codes are not yet perfectly set even for crack propagation alone with isotherm criteria [16, 17].

The one-dimensional model does not imply variation of the volume ($tr\varepsilon = 0$), and therefore, there is no change in temperature. Thus, the mechanical and thermal equations are uncoupled in the entire structure with the introduction of a concentrated heat source D at the crack-tip.

4.1 Mechanics Equation

The system is of a double beam cantilever (DCB) type, and it is subjected to opening efforts at its left extremities (Fig.4). The system has a prefissure of length a_0 . We need to determine the dissipation D at position $a(t)$ and speed $\dot{a}(t)$ owing to this crack. Because of the symmetry of the loading and geometry, we study only the upper part of the beam of section S and mass density ρ .

The one-dimensional problem involves the following considerations:

- a space variable: x ,
- a kinematic field: $u(x,t)$, transverse displacement,
- a stress component: $\tau(x,t)$, sharp effort.

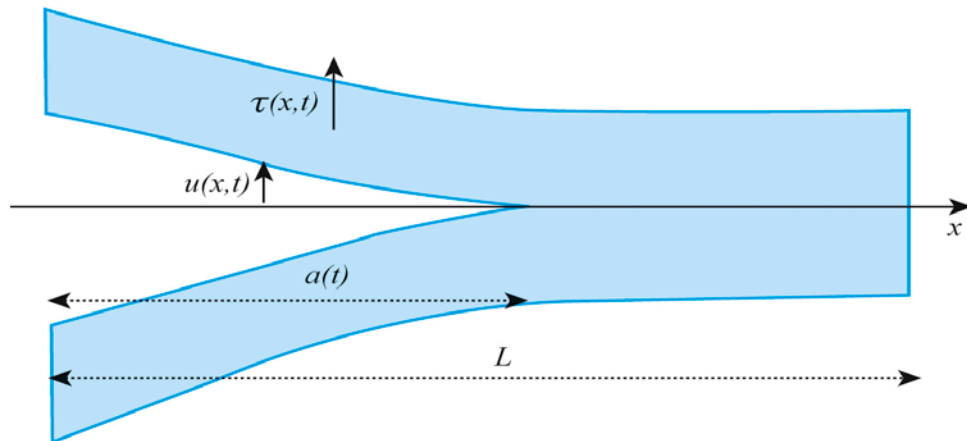


Fig.4 One-dimensional modelling.

4.1.1 Structural Behaviour

Motion equation

While considering that the system does not undergo a voluminal effort, the motion equations reduced to this kinematics lead to:

$$\frac{\partial \tau}{\partial x}(x, t) = \rho S \frac{\partial^2 u}{\partial t^2}(x, t) \quad (4.1)$$

Elastic constitutive law

The relation of the linear elastic constitutive law limited to one-dimensional kinematics is reduced to:

$$\tau(x, t) = \mu S \frac{\partial u}{\partial x}(x, t) \quad (4.2)$$

The modulus of elasticity μ represents the relationship between shearing and distortion. Only the behaviour in shearing is thus active.

Wave equation

From equations (4.1) and (4.2), we obtain the wave equation on $u(x, t)$, where $c = \sqrt{\frac{\mu}{\rho}}$ is the wave celerity in this medium:

$$c^2 \frac{\partial^2 u}{\partial x^2}(x, t) - \frac{\partial^2 u}{\partial t^2}(x, t) = 0 \quad (4.3)$$

of the general solution

$$u(x, t) = f(x - ct) + g(x + ct) \quad (4.4)$$

under the additional conditions defined below.

Initial conditions

The beam is initially assumed to be resting and to have a prefissure:

$$\begin{cases} u(x, t = 0) = 0 & \forall x \\ a(t = 0) = a_0 \end{cases} \quad (4.5)$$

Boundary conditions

A transverse load $F(t)$ is applied at the extremity $x = 0$ of the beam; at the same time, owing to wave propagation and the one-dimensional characteristic, the crack-tip imposes an embedding condition:

$$\begin{cases} \tau(x = 0, t) = -F(x, t) \\ u(x = a(t)) = 0 \end{cases} \quad (4.6)$$

This latter term is important because it is mobile: $a(t)$ evolves over time.

4.1.2 Fracture Parameters

Energy balance

To define the propagation criteria, we study the energy balance of the system and obtain parameters that can characterize the cracking. For this purpose, we write the energy balance of the closed system made up of the beam in its entirety from $x = 0$ to $x = L$:

$$\dot{\Psi}_{elas} + \dot{K} + D = P_{ext} \quad (4.7)$$

where

- $\dot{\Psi}_{elas} = \frac{d}{dt} \int_0^L \frac{1}{2} \frac{\tau^2}{\mu S} dx$: power associated with the elastic potential energy,
- $\dot{K} = \frac{d}{dt} \int_0^L \frac{1}{2} \rho S \dot{u}^2 dx$: power associated with the kinetic energy,
- D : power dissipated by the fracture,
- $P_{ext} = F(t) \cdot \dot{u}(x = 0, t)$: total power of the external efforts.

We show that the dissipated power D by the crack-tip is [14]

$$D = \frac{1}{2} \dot{a} \frac{\tau^2(a(t), t)}{\mu S} \left(1 - \frac{\dot{a}^2}{c^2} \right) \quad (4.8)$$

Fracture energy

The dissipation D in the crack-tip breaks up (2.13) into:

$$D = \dot{a} G \quad (4.9)$$

where G is the fracture energy [3]. From (4.8), it is shown to be:

$$G = \frac{1}{2} \frac{\tau^2(a(t), t)}{\mu S} \left(1 - \frac{\dot{a}^2}{c^2} \right) \quad (4.10)$$

G , being positive (2.13), leads to a theoretical limit of the propagation velocity, $\dot{a}(t) \leq c$.

In addition, the shock relation in the crack-tip results in:

$$\tau^+ = \tau^- \left(1 - \frac{\dot{a}^2}{c^2} \right) \quad (4.11)$$

where τ^+ and τ^- respectively denote the shearing ahead and behind the crack-tip.

Consequently, the fracture energy can be represented as:

$$G = \frac{1}{2} \frac{\tau^-}{\mu S} \tau^+ = \varepsilon^- \tau^+ \quad (4.12)$$

and can thus be identified as the product of the deformation factor ε^- and the stress factor τ^+ . This

expression is comparable with the Irwin formula [18], $G = \frac{k+1}{8\mu} K^\sigma K^u$.

4.2 Thermomechanical Coupling Aspect

4.2.1 Temperature Field at Crack-tip

The problem to be solved contains only a nonhomogeneity, and the internal source Φ has the following form:

$$k S \Delta T - \rho c S \dot{T} = \Phi \quad \text{with} \quad \Phi = \dot{a} G \delta(x = a(t)) \quad (4.13)$$

that we can resolve by, among others [19, 20], the impulse method (punctual source, instantaneous).

Indeed, if $T_\delta(x, t)$ is the response to the Dirac impulse, the solution $T(x, t)$ is given by

$$T(x, t) = T_\delta * f = \int_0^t T_\delta(t - \zeta) f(\zeta) d\zeta \quad \text{with} \quad f(t) \text{ a heat source} \quad (4.14)$$

For a propagating crack, the source is defined by $f(t) = G \dot{a}(t)$, and it is mobile from:

$$T(x, t) = \int_0^t T_\delta(x - a(\zeta), t - \zeta) G \dot{a}(\zeta) d\zeta \quad (4.15)$$

Resolution

The response to the Dirac impulse $T_\delta(x, t)$ in space and at time $t = 0$, $\delta(x = a(t)) \delta(t)$, is:

$$T_\delta(x, t) = \frac{1}{2\sqrt{\pi} S \sqrt{\rho c k} \sqrt{t}} e^{-\frac{\rho c x^2}{k 4t}} \quad (4.16)$$

Thus, the solution $T(x, t)$ is:

$$T(x,t) = \int_0^t \frac{1}{2\sqrt{\pi} S \sqrt{\rho c k} \sqrt{(t-\zeta)}} e^{-\frac{\rho c [x-a(\zeta)]^2}{k 4(t-\zeta)}} G \dot{a}(\zeta) d\zeta \quad (4.17)$$

This expression does not admit an analytical response even for a constant crack propagation velocity.

However, we can numerically integrate it with, for example, $k = \rho = c = S = 1$ (adimensional solution). Fig.5 shows the temperature profile at $x = 0$ with t variable. We note a convergence toward a constant temperature, $T = \frac{1}{2}$.

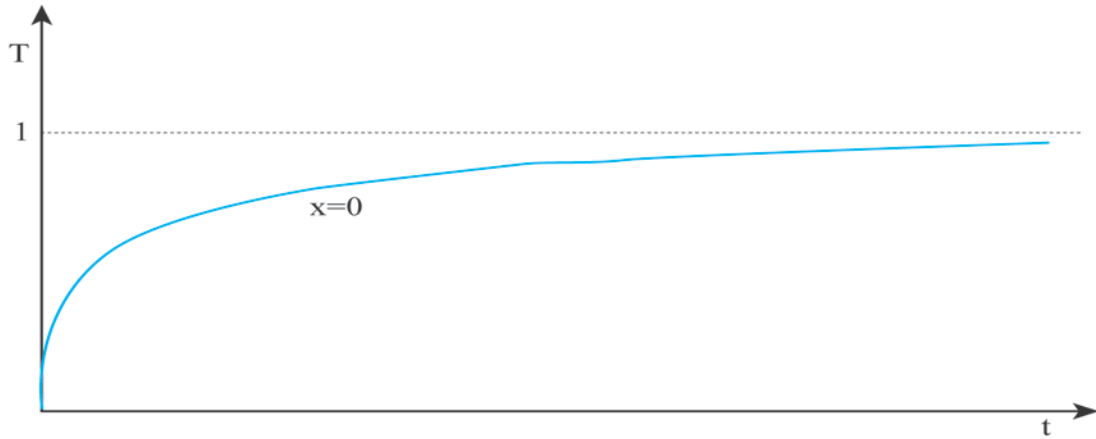


Fig.5 Adimensional solution of temperature at origin.

Furthermore, Fig.6 shows numerical solutions with $x = (1, 2, \dots)$ and t variable. We once again note a convergence at $t \rightarrow \infty$ but with temperature peaks at the moments of the passage of the crack to the considered X-coordinates.

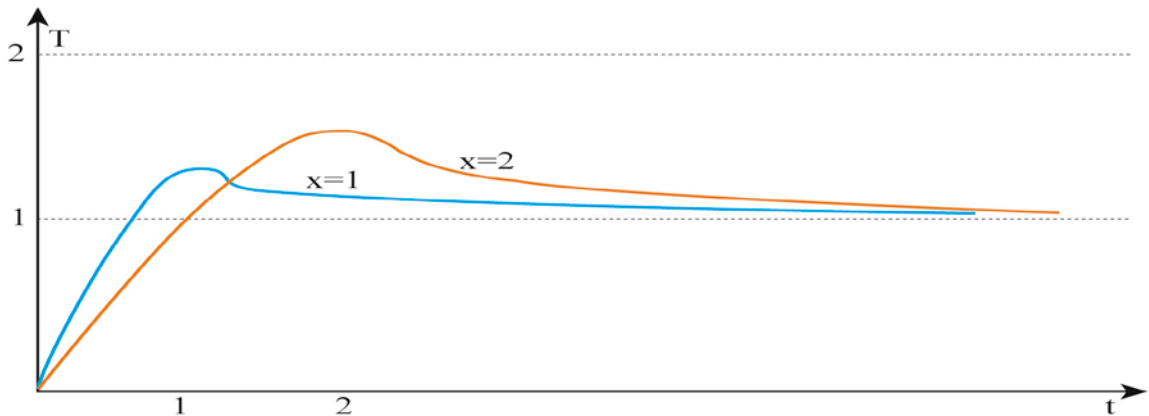


Fig.6 Adimensional solution of temperature in $x = (1, 2, \dots)$.

4.2.2 Fracture Process

To study the influence of temperature on crack propagation, it is thus necessary to precisely define a fracture criterion. Here, we choose the fracture energy G and its critical value G_c .

The fracture energy G is related to the strain and the stress at the crack-tip (4.12). Then, the propagation criterion starting from the critical fracture energy G_c is:

$$\left\{ \begin{array}{l} G = \frac{4}{\mu S} F^2(x-ct) \cdot \frac{1-\dot{a}}{1+\frac{\dot{a}}{c}} < G_c \Rightarrow \dot{a}(t) = 0 \\ G = \frac{4}{\mu S} F^2(x-ct) \cdot \frac{1-\dot{a}}{1+\frac{\dot{a}}{c}} = G_c \Rightarrow \dot{a}(t) > 0 \end{array} \right. \quad (4.18)$$

from which the resolution of a nonlinear differential equation of order I implies $a(t)$ (Fig.7).

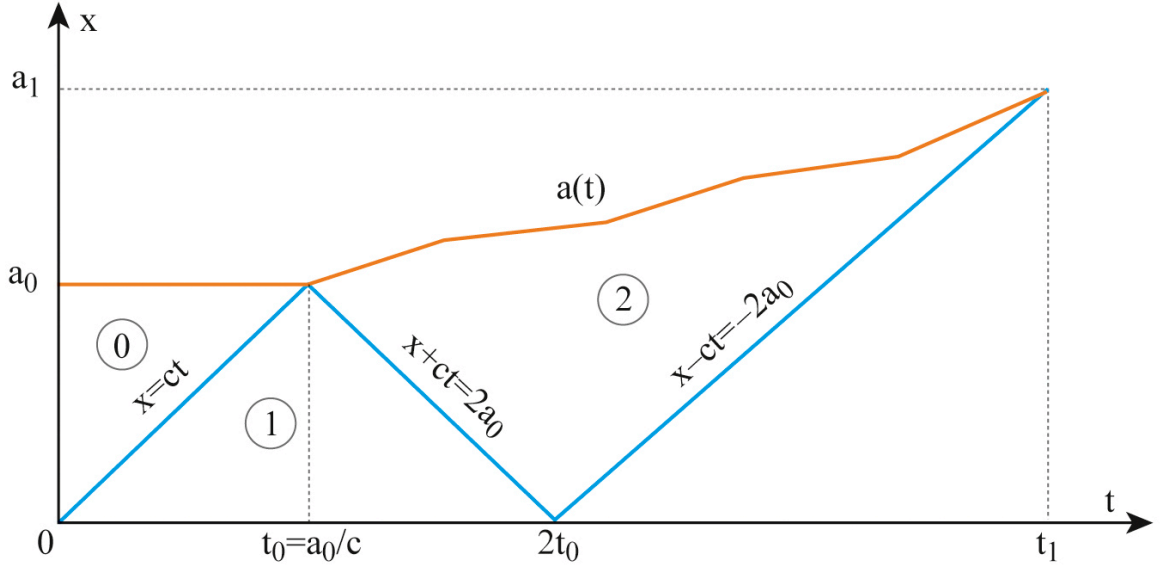


Fig.7 Arrival of the wavefront at the crack-tip and propagation.

For fracture, what interests us more particularly is the temperature immediately ahead of the crack-tip, as this temperature will define the properties of the resistance where the crack will be prolonged. The solution is regular (not temperature singularity at the crack-tip), and the temperature T_A at the crack-tip is expressed as:

$$T_A(t) = \int_0^t \frac{1}{2\sqrt{\pi} S \sqrt{\rho c k} \sqrt{(t-\zeta)}} e^{-\frac{\rho c [a(t)-a(\zeta)]^2}{k 4(t-\zeta)}} G \dot{a}(\zeta) d\zeta \quad (4.19)$$

If G and \dot{a} are constant, (4.19) is analytically integrated, and we find:

$$T_A(t) = \frac{G}{\rho c S} \operatorname{erf} \left(\frac{\dot{a}}{2} \sqrt{\frac{\rho c}{k} t} \right) \quad (4.20)$$

with $\operatorname{erf} z = \frac{2}{\sqrt{\pi}} \int_0^z e^{-\xi^2} d\xi$ (error function) and a limit at $t \rightarrow \infty$, $T_{A_{lim}}$, which is given by:

$$T_{A_{lim}} = \frac{G}{\rho c S} \quad (4.21)$$

This limiting temperature is two times the limit values for fixed x (Fig.8).

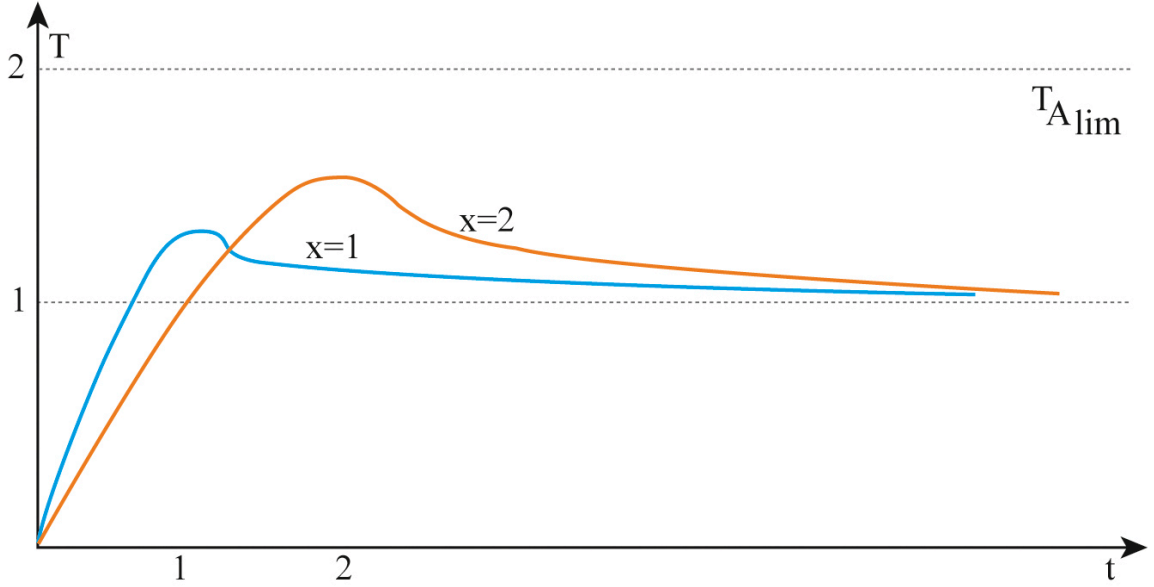


Fig.8 Adimensional solution of limiting temperature.

Furthermore, we deduce the characteristic time t_{car} required to reach this limiting temperature:

$$t_{car} = \frac{0.91 k}{\rho c \dot{a}^2} \quad (4.22)$$

If this time is very small, the temperature at the crack-tip will be given directly by the limit and will depend linearly on G , which can vary over longer times.

For example, on a bar of dimension $L = 0,35 m$ and $S = 2.10^{-4} cm^2$, we obtain the following values:

Table 2 Characteristic time and limiting temperature for steel and polyethylene.

	$\dot{a} [m.s^{-1}]$	$G[Pa.m]$	$T_{car}[s]$	$T_{A_{lim}}[^{\circ}C]$
Steel	800.00	468.75	$1.58 \cdot 10^{-11}$	62.00
Polyethylene	100.00	4,200.00	$1.94 \cdot 10^{-11}$	13.00

These values are representative only of the considered example because the solution strongly depends on the chosen parameters.

If t_{car} is very large, then complex coupling occurs during propagation. The temperature will increase with the crack position. Thus, even if G and \dot{a} are constant, the temperature will regularly increase, and therefore, it is possible to reach a thermal transition that will modify the propagation criterion.

To study this effect, it is necessary to first define all the relations between the criterion and the temperature; however, it is not very probable to obtain an analytical expression of the propagation even with a simple dependence.

For example, in the case of a bar impacted by another bar, the loading in effort is constant, and the equation of propagation is written as:

$$\frac{\dot{a}}{c} = \frac{\frac{F^2}{\mu S} - \frac{G_c}{4}}{\frac{F^2}{\mu S} + \frac{G_c}{4}} \quad (4.23)$$

We find a simple relation between \dot{a} and G_c . Nothing prevents variations of G_c over time, with the crack adapting to the speed (as opposed to an explicit dependence on time).

Thus, if the criterion of propagation with respect to the transition temperature T_c can be expressed as, for example,

$$\begin{cases} T < T_c & \Rightarrow G = G_c \\ T > T_c & \Rightarrow G = 2 G_c \end{cases} \quad (4.24)$$

the equation of propagation becomes:

$$\frac{\dot{a}}{c} = \frac{\frac{F^2}{\mu S} - \frac{G_c}{2}}{\frac{F^2}{\mu S} + \frac{G_c}{2}} \quad (4.25)$$

Assuming that the relation between T and G is always given by the limit reached instantaneously (4.21), T increases and is given by $2 T_c$ for $G = 2 G_c$:

$$T = \frac{2 G_c}{\rho c S} > T_c \quad (4.26)$$

When G reaches $2 G_c$, \dot{a} can be zero; this corresponds to the arrest of crack propagation. Then, the temperature decreases, involving a decrease in G_c and thus a possible reinitiation of crack propagation. There is thus an equilibrium regime with slowed-down propagation.

If the crack tends to stop, the temperature will be blocked at T_c , G_c will be fixed at the value corresponding to T_c (4.21), and \dot{a} can be deduced from G_c .

If \dot{a} is null again, then the propagation must be slow with a possibility of heat diffusion to remain under T_c .

In summary, the general analysis of the fracture process can be represented as shown in Fig.9.

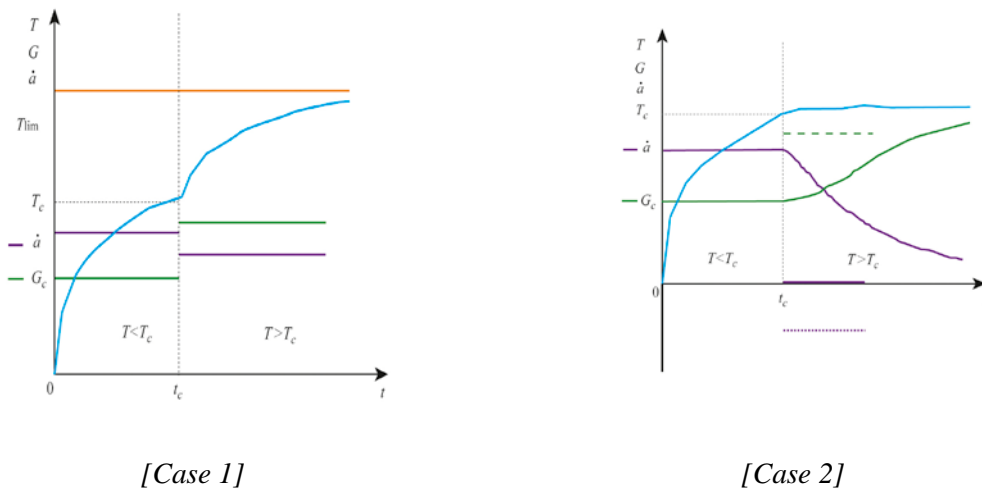


Fig.9 Propagation criterion with respect to the transition temperature T_c .

This one-dimensional modelling of thermomechanical coupling in dynamic fracture is useful for calculating the orders of magnitude, temperature, and characteristic time and for evaluating the effect of temperature on crack propagation with temperature-dependent criteria.

5. Conclusions

This study proposes an analytical model for thermal fields that combines crack energy flow with a heat equation using thermomechanical coupling. A methodology is proposed for analysing thermal fields.

The mechanical fields approach an equilibrium state for a short time during crack propagation until those at the crack tip are affected by the boundary. The temperature field developed in thermomechanically coupled problems can provide information about the energy consumption in the material, and techniques such as an instant measurement of the temperature field can serve as a powerful tool for understanding the dynamic fracture.

This study does not fully solve the problem of thermomechanical coupling in dynamic fracture. It might model dynamic elastoplastic rupture more finely by introducing a thermoviscoplastic effect because the viscosity decreases with temperature. Confined plasticity problems are taken into account if the crack energy flow is interpreted in a more general manner as the power consumed by unit advancement of a crack. In the future, it might be useful to more precisely study the effects of coupling in the propagation phase in a one-dimensional model.

References

1. Guduru P.R., Zehnder A.T., Rosakis A.J. and Ravichandran G., 'Dynamic full field measurements of crack tip temperatures', *Engng. Fract. Mech.*, **68** (2001), 1535 – 1556.
2. Rittel D., 'Thermomechanical aspects of dynamics crack initiation', *Int. J. Fract.*, **99** (1998), 199 – 209.
3. Bui H.D., Ehrlacher A. and Nguyen Q.S., 'Thermomechanical couplings in fracture mechanics', *Thermomechanical Couplings in Solids*, Elsevier Science Publishers, New York, 1986, 327 – 341.
4. Soumahoro Z., 'Study of thermomechanical coupling in dynamic crack propagation problems', *PhD Thesis, Ecole Polytechnique (France)*, 2005.
5. Freund L.B., 'Dynamic fracture mechanics', Cambridge University Press, Cambridge, 1990.
6. Döll W., 'An experimental study of the heat generated in the plastic region of a running crack in different polymeric materials', *Engng. Fract. Mech.*, **5** (1973), 259 – 268.
7. Shockey D.A., Kalthoff J.F., Klemm W. and Winkler S., 'Simultaneous measurements of stress intensity

- and toughness for fast running cracks in steel', *J. Exp. Mech.*, **40** (1983), 140 – 152.
8. Fuller K.N.G., Fox P.G. and Field J.E., 'The temperature rise at the tip of fast-moving cracks in glassy polymers', *Proc. Roy. Soc. Lond.*, **341** (1975), 537 – 557.
 9. Weichert R. and Schönert K., 'Heat generation at the tip of moving crack', *J. Mech. Phys. Solids*, **26** (1978), 151 – 161.
 10. Weichert R. and Schönert K., 'On the temperature rise at the tip of a fast running crack', *J. Mech. Phys. Solids*, **22** (1978), 127 – 133.
 11. Rice J.R. and Levy N., 'Local heating by plastic deformation at a crack tip', *Physics of Strength and Plasticity*, MIT Press, Cambridge, 1969, 277 – 293.
 12. Salençon J., 'Mécanique des milieux continus', Les Editions de l'Ecole Polytechnique, France, 2001.
 13. Ehrlacher A., 'Contribution à l'étude thermodynamique de la progression de fissure et à la mécanique de l'endommagement brutal', *Thèse de Doctorat d'Etat, Université Pierre et Marie Curie, Paris*, 1985.
 14. Carin T., 'Modélisation de la propagation dynamique de fissure', *Thèse de Doctorat, Ecole Nationale des Ponts et Chaussées, France*, 2000.
 15. Kallivayalil J.A. and Zehnder A.T., 'Measurement of the temperature field induced by dynamic crack growth in Beta-C titanium', *Int. J. Fract.*, **66** (1994), 99 – 120.
 16. Williams J.G., 'A global energy analysis of impact loaded bi-material strips', *Engng. Fract. Mech.*, **6** (2005), 813 – 826.
 17. Williams J.G. and Pavan A., 'Fracture of polymers, composites and adhesives', Elsevier Science Ltd., Oxford, 2000.
 18. Irwin G.R., 'Analysis of stresses and strains near the end of a crack traversing a plate', *J. Appl. Mech.*, **3** (1957), 361 – 364.
 19. Carslaw H.S. and Jaeger J.C., 'Conduction of Heat in Solids', Oxford University Press, England, 1959.
 20. Boley B.A., 'Theory of thermal stresses', J. Wiley and Sons, New York, 1960.